Direct observation of the LO phonon bottleneck in wide GaAs/$Al_xGa_{1-x}As$ quantum wells

B. N. Murdin*
FOM-Institute ''Rijnhuizen,'' P.O. Box 1207, 3430 BE Nieuwegein, The Netherlands

W. Heiss
Institut für Festkörperelektronik, T. U. Wien, A-1040 Wien, Austria

C. J. G. M. Langerak
FOM-Institute ''Rijnhuizen,'' P.O. Box 1207, 3430 BE Nieuwegein, The Netherlands
and Department of Physics, Heriot-Watt University, Edinburgh EH14 4AS, United Kingdom

S.-C. Lee and I. Galbraith
Department of Physics, Heriot-Watt University, Edinburgh EH14 4AS, United Kingdom

G. Strasser and E. Gornik
Institut für Festkörperelektronik, T. U. Wien, A-1040 Wien, Austria

M. Helm
Institut für Halbleiterphysik, Universität Linz, A-4040 Linz, Austria

C. R. Pidgeon
Department of Physics, Heriot-Watt University, Edinburgh EH14 4AS, United Kingdom
(Received 25 September 1996)

We report the direct observation of a bottleneck in electron cooling in wide GaAs quantum wells. Intersubband lifetimes τ and their dependence on intensity, lattice temperature T_L, and well width have been measured using a ps excite-probe technique in wells with subband separation less than the longitudinal optical (LO) phonon energy. Above an electron temperature of about $T_e=35$ K the lifetime depends on T_e and is determined by LO-phonon emission. Below this bottleneck temperature acoustic phonons dominate the plasma cooling. An energy balance model of these interactions, with no adjustable parameters, gives good agreement with our results. At electron temperatures below 35 K we determine $\tau=500$ and 200 ps for samples of subband energy 19.5 and 26.6 meV, respectively. [S0163-1829(97)04908-4]

I. INTRODUCTION

The knowledge of semiconductor quantum-well intersubband lifetimes and relaxation processes is of fundamental interest and is crucial for the design of emitters and detectors based on these systems.[1] There are two regimes of hot electron relaxation that can be distinguished in semiconductor heterostructures, depending on whether the electron energy is larger or smaller than the longitudinal optical (LO) phonon energy (36.7 meV in GaAs). For the former case, many experiments aimed at the determination of the intersubband lifetime have been performed in the last ten years,[2–7] giving a result of the order of 0.3 ps (Refs. 4–6) in agreement with LO-phonon emission theory. For the latter case a variety of relaxation times between 15 and 1200 ps have been reported,[7–14] measured with several different techniques on samples of various well widths, doping profiles, and concentrations. These longer lifetimes have also recently been discussed in terms of LO-phonon emission at elevated electron temperatures,[15] where the excited electron temperature was not calculated but used as a fitting parameter. In addition it has been shown elsewhere that, for an electrically heated two-dimensional electron gas, energy relaxation is dominated by acoustic phonon emission below an electron temperature of 40 K and by optical phonon emission above this temperature.[16,17]

Until recently, most experiments were performed by time-resolved, ultrafast interband spectroscopy using excitation of electron-hole pairs in undoped samples.[6–9] In such measurements care has to be taken to properly consider the dynamics of the holes. Other complications arise, because excitation of electrons into the second subband is always accompanied by excitation into the first subband at a higher k vector and additionally the excitation density is not very well known. These problems can be avoided by using intersubband spectroscopy in doped quantum wells. Such experiments have been performed above the LO-phonon energy with mid-IR picosecond laser systems[2] and by steady-state absorption saturation measurements with CO_2 lasers.[3,4] The latter method has also been used below the LO phonon energy with a quasi-cw free-electron laser.[12,13] Steady-state saturation measurements, however, require a nontrivial analysis that involves very accurate calibration of the laser intensity in the sample, along with several other sample parameters and their dependences, all of which directly influence the extracted lifetime.

We report the direct observation of a bottleneck in electron cooling in wide $GaAs/Al_{0.3}Ga_{0.7}As$ multiple quantum-well structures, using the excite-probe technique with a far-infrared free electron laser (FEL). The samples are designed to have the transition energy between the two lowest subbands less than the LO-phonon energy. We have also developed a numerical model, with no adjustable parameters, based on the energy balance of the system, i.e., energy gain through photons and energy loss through optical and acoustic phonons. This allows us to explain quantitatively the lifetimes and their dependence on laser intensity, well width, and lattice temperature for both pulsed, time-resolved, and cw measurements.

II. EXPERIMENT

The two samples consisted of ten periods of a simple square quantum well of $GaAs/Al_{0.3}Ga_{0.7}As$, modulation doped to 2.0×10^{11} cm^{-2} per well with a (depolarization shifted[12,13]) intersubband energy of 19.5 meV (sample *A*, well width 30 nm) and 26.6 meV (sample *B*, well width 24 nm), respectively. In order to provide an electric field component perpendicular to the layers a metallic grating (Ti/Au, 8 μm period) was deposited on the structure, enabling excitation of intersubband transitions by normal incidence radiation. An absorption amounting to a transmission decrease of about 25% was observed using a Fourier transform spectrometer. The grating also acted as a gate to modulate the carrier concentration in the wells, greatly enhancing the sensitivity of the measurement.

FELIX (free-electron laser for infrared experiments) delivers so-called ''macropulses'' with a length of 5–20 μs at a maximum repetition rate of 5 Hz.[18] Each macropulse consists of a train of ''micropulses'' with a spacing that can be set at either 1 or 40 ns. In our case the latter setting was used. The sample was mounted on a 2-mm pinhole in a liquid-helium cryostat. The pump radiation was directed onto it via a focusing mirror, which brought the spot size down from 15 mm (half power diameter) to 5 mm. A small part of the beam, the probe, was diverted with a mylar beam splitter into a movable retroreflector, which acted as a delay line. The probe was then directed unfocused onto the sample at an angle of 15° to the pump. The peak pump and probe irradiances were corrected for losses due to beam splitters, windows, and grating. The change in transmission of the probe as the absorption recovers was measured as a function of delay with a sensitive liquid-helium-cooled Ge:Ga detector. In addition the probe beam was monitored with a second beam splitter and detector, so that drift in the laser power could be divided out.

III. THEORY

The recombination processes that compete in the carrier dynamics of these structures are (a) the electron-electron or Auger collisions, a very fast (sub-ps) thermalizing process that does not contribute to net energy loss of the electron gas; (b) ionized impurity scattering, an elastic thermalizing process that may be very fast (ps), (c) longitudinal optical (LO) phonon emission, an energy-loss mechanism known to occur on a subpicosecond time scale; and (d) acoustic phonon scattering, energy loss on a several hundred picosecond time scale. The dynamics as an electron is excited and then relaxed from the second subband to the bottom of the first subband are a complicated mixture of these processes and can be described in detail using Monte Carlo simulations.[19] However, in this work we present a rate equation model that has the benefit of having no fitting parameters, and that accounts for the experimental results at delay times after the passage of the pump pulse.

It is not necessarily the fastest single mechanism that ''dominates'' the relaxation. We note that for a combination of scattering processes in parallel, the fastest channel will be dominant. However, if the dominant channel is made up of a sequence of more than one process, then of these processes it will be the slowest that determines the experimentally measured lifetime. The primary pathways that are to be expected in our wide wells are thermalization of the electron gas by the fast elastic processes, carrier-carrier and ionized impurity scattering, followed by either LO-phonon emission by those carriers that now have sufficient energy, or by acoustic phonon emission. For these pathways the phonon emission is the slowest step, which thus dominates the observed relaxation.

We assume that the electron-electron and ionized impurity scattering instantaneously drive the electrons in all subbands into thermal equilibrium, i.e., into a single Fermi distribution with one well-defined value of T_e, and one chemical potential μ at all times. The Monte Carlo calculations[19] show that this is a good approximation for times a few ps after the excitation. We show that this model gives excellent agreement with the experimentally observed intensity and well width dependences, and enables us to understand the temperature dependence of the recombination rates.

In order to calculate T_e (and μ) as a function of time during and after the excitation pulse, we calculate the change in the total energy of the electron gas, $E_{\rm tot}$ from the rate equation (keeping the total carrier density fixed). Energy input comes only from photon absorption and the energy loss is due to phonon emission:

$$\frac{dE_{\rm tot}}{dt}=\hbar\omega_{21}W_g-P_{\rm LO}-P_A. \tag{1}$$

The first term is the net generation rate due to absorption and stimulated emission of photons, $W_g=(N_1-N_2)\sigma I/\hbar\omega_{21}$, where N_1 and N_2 are the carrier concentrations in the first and second subband, σ is the effective absorption cross section (including the radiation coupling efficiency), I is the pump laser intensity, and $\hbar\omega_{21}$ is intersubband transition energy. We determine σ and N_2 directly from the probe transmission in the absence (i.e., small signal) and presence of the pump, respectively. The second and third terms are the total energy-loss rates (i.e., summing over all initial and final states) due to LO and acoustic phonons, respectively.

To calculate the LO-phonon energy-loss rate, $P_{\rm LO}=\hbar\omega_{\rm LO}W_{\rm LO}$ (where $\hbar\omega_{\rm LO}$ is the LO-phonon energy), we include only the dominant polar optical phonon scattering, starting from the Fröhlich electron–LO-phonon coupling. We integrate over final states to find the one-electron scattering rate, and then integrate over the Fermi distribution of carriers to give the total LO-phonon scattering rate $W_{\rm LO}(T_e)$.[15] $W_{\rm LO}$ is a function of the lattice temperature T_L

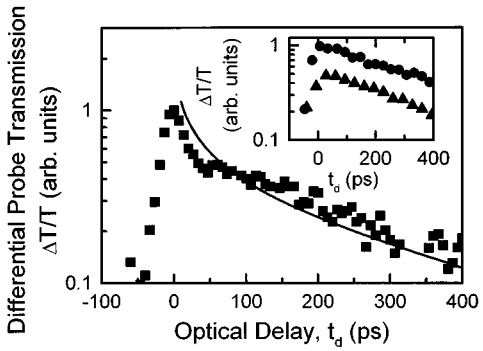

FIG. 1. Differential probe transmission vs optical delay at $T_L=5$ K for sample A at high internal intensity ($I=6$ kW/cm^2, pulse width 15 ps). Experimental results (squares) and theory (solid line). Inset: results for different peak intensities taken with a pulse width 50 ps: $I=40$ W/cm^2 (circles) and 10 W/cm^2 (triangles) also at $T_L=5$ K. The low intensity curves have been shifted for clarity.

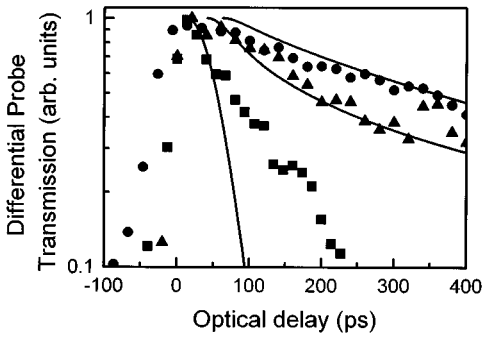

FIG. 2. Differential probe transmission for the sample A (19.5 meV) vs optical delay between excite and probe pulses. Experimental results are shown for three different lattice temperatures, $T_L=5$ K (circles), 25 K (triangles), and 45 K (squares) at a fixed internal peak excitation intensity $I=40$ W/cm^2 and pulse duration of 50 ps. Also shown are the calculated results (solid lines).

via the LO-phonon occupation number, and of the LO-phonon energy. It is also a function of the subband separation and of the detailed quantum-well structure via a matrix element $G_{i,f}=\langle\psi_i|\exp(iq_z z)|\psi_f\rangle$, where q_z is the z component of the phonon wave vector. We have included in our calculations two subbands and both intersubband and intrasubband emission and absorption.

The net (i.e., including emission and absorption) piezoelectric and deformation potential acoustic phonon power losses are proportional to (T_e-T_L) for the intrasubband loss in the degenerate approximation.[16] The total, P_A, is only significant by comparison with $\hbar\omega_{\rm LO}W_{\rm LO}$ at low electron temperatures where our samples are indeed nearly degenerate. Also when T_e is low there are very few carriers in the second subband, so that the intrasubband cooling dominates the acoustic phonon scattering contribution to our measured relaxation rate.

IV. RESULTS AND DISCUSSION

In a high intensity excite-probe experiment, Fig. 1, the differential transmission was measured for sample A at a lattice temperature of $T_L=5$ K. An initial fast decay rate with a lifetime τ around 45 ps was observed, consistent with our previous measurement[10] on a similar sample under similar conditions (N.B. the lifetime is determined simply from the slope of the logarithmic graph). The decay slows down rapidly until $\tau\sim500$ ps. This slower decay was not resolved above noise previously.[10] The pulse duration, corresponding to the resolution limit of the measurement, was measured to be 15 ps from the rising edge of the differential transmission. The rapidly changing slope associated with the change of τ is a consequence of a ''bottleneck'' in the emission of LO phonons. After the electron gas is heated by the excite pulse, a rapid cooling by LO phonons takes place. However, as the number of carriers above the LO-phonon energy drops the emission disappears, and the cooling is stopped. This occurs at an electron temperature around $T_e=35$ K, and all further cooling takes place by slow acoustic phonon emission. When the intensity, and therefore the electron heating, is reduced, the initial fast decay by LO-phonon emission disappears. Figure 1 (inset) shows the effect of reducing the intensity until only a small perturbation of the electron temperature is made, and further reduction in intensity has no effect.

Equation (1) is solved numerically for the FEL pulse to yield the time dependence of the population and thus the transmission change. The model results for the excite-probe transmission change versus delay time are shown in Fig. 1. We emphasize that all parameters used in the model have been independently determined. Since the model is only valid at times after the passage of the pump pulse, we only plot the theoretical curve in this regime for all cases. After the laser pulse has passed, the evolution of the decay rate is in very good agreement with the measurement, with the LO-phonon cooling rate slowing considerably over time.

In order to quantify more directly the effect of electron temperature on the cooling rate, we have performed low-intensity excite-probe measurements for sample A (19.5 meV) at a variety of lattice temperatures, shown in Fig. 2. At the lowest temperature ($T_L=5$ K), we find the relaxation time of 500($\pm$50) ps. There is little change in the decay rate at $T_L=25$ K. From 45 K upwards, as shown more clearly in Fig. 3, we see a rapid increase in the decay rate with increas-

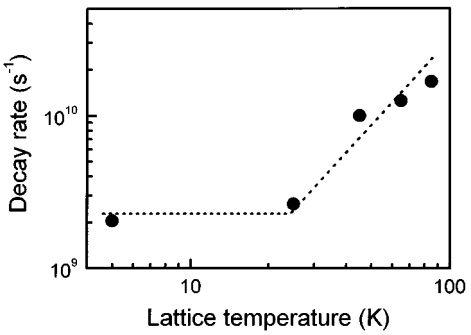

FIG. 3. Measured decay rate (circles) taken from the slope of the experimental differential transmission data (from Fig. 2, together with other T_L curves not shown), plotted as a function of lattice temperature. The size of the symbols represents the estimated error. The dotted line is a guide to the eye.

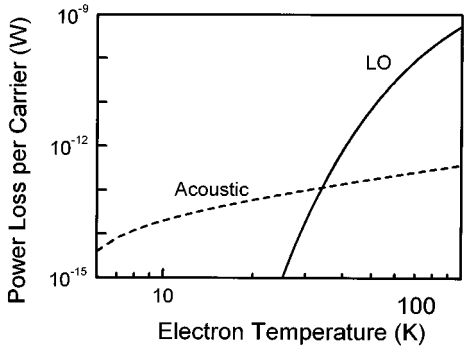

FIG. 4. Theoretical electron temperature dependence of the energy loss rates via LO (solid line) and acoustic phonons (dashed line). The crossover indicates the bottleneck electron temperature.

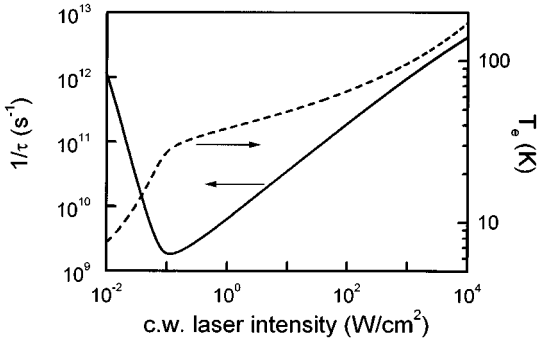

FIG. 6. Calculated inverse carrier lifetime (left axis) and excited electron temperature (right axis) vs laser intensity for cw (i.e., steady state) excitation. Sample parameters used are from Ref. 13.

ing temperature up to the resolution limit (determined to be ≈50 ps in this case). This constitutes a direct measurement of the *electron* temperature of 35±10 K. Since the acoustic phonon cooling depends only weakly on T_e, the lifetime is virtually unchanged for all lattice temperatures less than the bottleneck electron temperature. For higher lattice temperatures there are always sufficient electrons above the LO-phonon energy to allow fast electron cooling.

At 45 K (and above) the measured LO emission lifetime is longer than that given by the model (Fig. 2). This can be understood in terms of hot phonon effects, which reduce cooling rates by enhancing the reabsorption of LO phonons,[8] and are not included in our model. Figure 4 shows the calculated phonon cooling rates as a function of electron temperature for T_L=5 K, clearly indicating that the crossover from acoustic to LO-phonon-dominated cooling occurs at T_e=35 K, which agrees well with the lattice temperature at which we observe the bottleneck.

As a further check we have determined the dependence of relaxation rate on well width. Differential probe transmission versus delay measurements are shown in Fig. 5, for sample B, and compared to the decay curve for sample A under the same experimental conditions. A smaller measured lifetime of 200 ps is obtained for the higher energy sample B. Excellent agreement is obtained with the theory showing the expected increase of decay rate as the subband transition energy approaches the optical phonon energy (i.e., the lifetime is 500 ps for sample A and 200 ps for sample B).

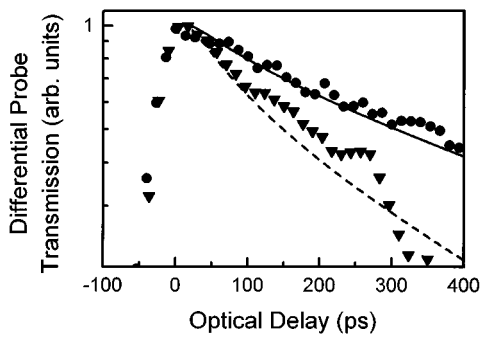

FIG. 5. Differential probe transmission versus optical delay at T_L=5 K for sample *A* [19.5 meV (circles)] and sample *B* [26.6 meV (triangles)]. Theoretical results are also shown (solid and dashed lines, respectively).

Within our model we can also explore the cw limit, and observe the effects of the LO-phonon bottleneck. By putting the rate equation (1) into the steady state we can find the electron temperature and therefore also N_2 as functions of cw laser intensity. Similarly, from the rate equation for the excited carrier concentration in a two-level model:

$$\frac{dN_2}{dt} = W_g - \frac{N_2}{\tau}, \tag{2}$$

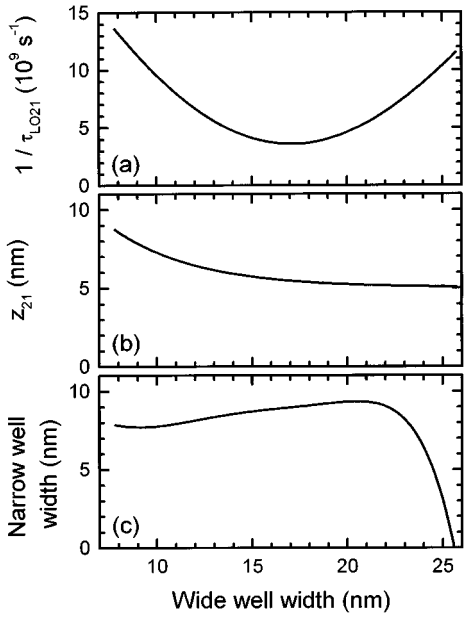

FIG. 7. Calculated recombination rate for LO-phonon emission for ASQW's obtained by moving the barrier position between the quantum wells from a symmetric to a strongly asymmetric structure. A central barrier width of 2 unit cells is assumed. (a) Recombination rate, $1/t_{\mathrm{LO21}}$ at 77 K, versus wide well width; (b) the optical transition dipole moment vs wide well width, as in (a); (c) the narrow well width was adjusted for each wide well width in order to maintain a fixed intersubband energy separation of E_{21}=20 meV as shown.

we find the apparent lifetime τ is given by

$$\frac{1}{\tau}=\frac{W_g}{N_2}=\left(\frac{N_1-N_2}{N_2}\right)\frac{\sigma I}{\hbar\omega_{21}}. \tag{3}$$

By contrast with the pulsed results above, a very strong intensity dependence of $1/\tau$ and T_e calculated from Eq. (3) is found as is shown in Fig. 6. The turning points in both are due to the change in the dominant relaxation mechanism at the bottleneck temperature, 35 K. The initial fast (superlinear) rise in T_e with intensity is due to the ease of overcoming the slow acoustic phonon emission. This has the effect [from Eq. (3)] of a fall in $1/\tau$, a similar behavior has been observed in transport measurements at very low energy electrical excitation.[16] At electron temperatures above the bottleneck temperature the LO phonons become more important, and it becomes harder to raise N_2 by increasing the intensity. N_2 is then sublinear in I and therefore $1/\tau$ rises again. In order to compare actual experimental results with the calculations, we have used for Fig. 6 the sample parameters and experimental conditions of Ref. 13. The turning point (at $I=10^{-1}$ W/cm^2 and $1/\tau=10^9$ s) is in good absolute agreement with a low-intensity knee in these measurements, and our high-intensity rise also is consistent with the experimental result.

Finally, we add that our model predicts that the bottleneck temperature for a given subband transition energy—and therefore also the lifetime at the bottleneck temperature—depends on the matrix element G, and the carrier concentration. Since G may be altered by engineering the band structure (e.g., in asymmetric coupled quantum wells) without necessarily changing the intersubband energy, this opens up the possibility of lifetime design. If we arbitrarily define a figure of merit, $[\tau_{\rm LO}\,(T_e=77\ {\rm K})]^{-1}$, then this should be minimized to find the structures with greatest suitability for laser devices. For example, taking a subband separation of 20 meV, we find significant improvement for the asymmetric coupled quantum well (ACQW) over the simple quantum well. As a typical, but by no means optimized, example, we show a computation in Fig. 7 of the relaxation rate as a function of wide well width. For an ACQW system with constant barrier width 1.12 nm, we varied the wide well width from 26 down to 7 nm while adjusting the narrow well width to maintain a constant optical transition energy of $E_{21}=20$ meV. We see that the relaxation rate can be changed by a factor of about 3. The matrix element for the optical transition, z_{21}, remains approximately constant in this range.

V. SUMMARY AND CONCLUSION

In summary, with a pump-probe technique we have directly measured the electron dynamics in wide GaAs quantum wells with the subband separation less than the LO-phonon energy. With the aid of a simple energy balance model of optical absorption and optic and acoustic phonon cooling, we have calculated the electron temperature and excited carrier concentration as a function of delay time after the pulse, and hence determined the relaxation time for different quantum-well structures. At temperatures below 35 K we determine $\tau=500$ and 200 ps for samples of subband energy 19.5 and 26.6 meV, respectively. At short delay times and high laser intensities we observe a rapidly changing decay rate. We have demonstrated a bottleneck in relaxation by LO-phonon emission, and shown that the relaxation rate depends critically on whether the electron temperature is above or below the bottleneck temperature. The rate equation calculation successfully accounts not only for these results, but also for others in the literature including those using cw excitation. In Table I we summarize the experimental and calculated lifetimes for the $2\rightarrow1$ intersubband transitions in wide GaAs/$Al_{1-x}Ga_xAs$ for the two samples of the present work, together with that of a previous study.[10] We also include our calculated results for the cw experiments of other workers.[12,13] It is very clear that for an electron temperature above 35K the lifetime is critically dependent on the electron temperature. In agreement with Lee, Galbraith, and Pidgeon,[15] we believe this accounts for the wide divergence of earlier results (Ref. 9: $\tau_{\rm expt}=570$ ps, $\tau_{\rm calc}=630$ ps with $T_e<35$ K; Ref. 7: $\tau_{\rm expt}=20$ ps, $\tau_{\rm calc}=21$ ps with $T_e=78$ K).

Finally, we have seen that the LO-phonon emission lifetime depends not only on the electron temperature but on asymmetric coupled well structure, opening up the possibility of lifetime design. By varying the barrier position between the two wells we have shown that significant improvements over the simple quantum well case are possible, up to a factor of three. Clearly the short lifetimes that we have demonstrated at high T_e will put a restriction upon new schemes for intersubband lasing, but one way of overcoming this might be additional structuring with dots or wires to reduce the LO-phonon emission. Future work should involve further iterations of the optimization procedure and investigation of other types of structure, with variation in the well depths, for example.

ACKNOWLEDGMENTS

We would like to acknowledge support by FOM (NL) in providing the necessary beamtime on FELIX, and highly ap-

TABLE I. Table of experimental and calculated lifetimes for the $2\rightarrow1$ intersubband transitions in wide GaAs/$Al_xGa_{1-x}As$ wells. Experimental parameters are also displayed.

Reference	ΔE_{21} (meV)	n_e (cm^{-2})	$T_{\rm lattice}$ (K)	T_e (K)	$\tau_{\rm expt}$ (ps)	$\tau_{\rm calc}$ (ps)
Present work	19.5	2.0×10^{11}	15	<25	500 ± 50	500
	26.6	2.0×10^{11}	15	<25	200 ± 30	200
Murdin *et al.* (Ref. 10)	18	1.5×10^{11}	10	50	40 ± 5	40
Heyman *et al.* (Refs. 13 and 14)	10.9	8×10^{10}	10	6	1.6 ns	750
	10.9	8×10^{10}	10	100	10	1

preciate the assistance of the FELIX staff, in particular Dr A.F.G. van der Meer. This work has been supported by EPSRC (UK), ''Gesellschaft fuer Mikroelektronik,'' the ''Bundesministerium fuer Wissenschaft, Verkehr unf Forschung,'' and an ''INTAS'' grant. One of us (C.J.G.M.L) is grateful for the financial support EPSRC and B.N.M. for the support of an EU-HCM. We acknowledge very useful conversations with Tony Vickers, and the contribution of *N* Nassar to the lifetime design computations.

*Present address: Department of Physics, University of Surrey, Guildford GU2 5XH, UK.

[1] J. Faist, F. Capasso, D. L. Sivco, C. Sirtori, A. L. Hutchinson, and A. Y. Cho, Science **264**, 553 (1994); J. Faist, F. Capasso, C. Sirtori, D. L. Sivco, J. N. Baillargeon, A. L. Hutchinson, S.-N. G. Chu, and A. L. Cho, Appl. Phys. Lett. **68**, 3680 (1996).

[2] A. Seilmeier, H. J. Hubner, G. Abstreiter, G. Weimann and W. Schlapp, Phys. Rev. Lett **59**, 1345 (1987); R. J. Bäuerle, T. Elsaesser, H. Lobentanzer, W. Stolz, and K. Ploog, Phys. Rev. B **38**, 4307 (1988); T. Elsaesser, R. J. Baurle, W. Kaiser, H. Lobentanzer, W. Stolz, and K. Ploog, Appl. Phys. Lett. **54**, 256 (1989).

[3] L. C. West and C. W. Roberts, in *Quantum Well Intersubband Transition Physics and Devices* (Kluwer Academic Publishers, Dordrecht, 1994), p. 501.

[4] F. H. Julien, J. M. Lourtioz, N. Herschlorn, D. Delacourt, J. P. Pocholle, M. Papuchon, R. Planel, and G. Le Roux, Appl. Phys. Lett. **53**, 116 (1988); **62**, 2289 (1993); D. Cui, Z. Chen, S. Pan, H. Lu, and G. Yang, Phys. Rev. B **47**, 6755 (1993).

[5] J. Faist, F. Capasso, C. Siortori, D. L. Sivco, A. L. Hutchinson, S-N. G. Chu, and A. Y. Cho, Appl. Phys. Lett. **63**, 1354 (1993); S. Hunsche *et al.*, Phys. Rev. B **50**, 5791 (1994).

[6] M. C. Tatham, J. F. Ryan, and C. T. Foxon, Phys. Rev. Lett. **63**, 1637 (1989).

[7] J. A. Levenson, G. Dolique, J. L. Oudar, and I. Abram, Phys. Rev. B **41**, 3688 (1990).

[8] K. Leo, W. W. Rühle, and K. Ploog, Phys. Rev. B **38**, 1947 (1988).

[9] D. Y. Oberli, D. R. Wake, M. V. Klein, J. Klem, T. Henderson, and H. Morkoc, Phys. Rev. Lett. **59**, 696 (1987).

[10] B. N. Murdin, G. M. H. Knippels, C. J. G. M. Langerak, A. F. G. van derMeer, C. R. Pidgeon, M. Helm, W. Heiss, K. Unterrainer, E. Gornik, K. K. Geerinck, N. J. Hovenier, and W. Th. Wenckebach, Semicond. Sci. Technol. **9**, 1554 (1994).

[11] J. Faist, F. Capasso, C. Sirtori, D. L. Sivco, A. Y. Chio, L. N. Pfeiffer, and K. W. West, Appl. Phys. Lett. **64**, 872 (1994).

[12] K. Craig, C. L. Felix, J. N. Heyman, A. G. Markelz, M. S. Sherwin, K. L. Campman, P. F. Hopkins, and A. C. Gossard, Phys. Rev. Lett. **76**, 2382 (1996).

[13] J. N. Heyman, K. Unterrainer, K. Craig, B. Galdrikian, M. S. Sherwin, K. L. Campman, P. F. Hopkins, and A. C. Gossard, Phys. Rev. Lett. **74**, 2682 (1995).

[14] J. N. Heyman, K. Unterrainer, K. Craig, J. Williams, M. S. Sherwin, K. Campman, P. F. Hopkijs, A. C. Gossard, B. N. Murdin, and C. J. G. M. Langerak, Appl. Phys. Lett. **63**, 3019 (1996).

[15] S-C. Lee, I. Galbraith, and C. R. Pidgeon, Phys. Rev. B **52**, 1874 (1995).

[16] M. E. Daniels, B. K. Ridley, and M. Emeny, Solid State Electron. **32**, 1207 (1989); N. Balkan, H. Celik, A. J. Vickers, and M. Cankurtaran, Phys. Rev. B **52**, 17 210 (1995).

[17] K. Hirakawa, M. Grayson, D. C. Tsui, and C. Kurdak, Phys. Rev. B **47**, 16 651 (1993).

[18] D. Oepts, A. F. G. van der Meer, and P. W. van Amersfoort, Infrared Phys Technol. **36**, 297 (1995).

[19] S. M. Goodnick and P. Lugli, Superlatt. Microstruct. **5**, 51 (1989); B. N. Murdin *et al.*, *ibid.*. **19**, 17 (1996).